

## Excitation and multiple dissociation of $^{12}\text{C}$ , $^{14}\text{N}$ , and $^{16}\text{O}$ projectiles in peripheral collisions at 32.5 MeV/nucleon

J. Pouliot,<sup>(1)\*</sup> Y. Chan,<sup>(1)</sup> D. E. DiGregorio,<sup>(1)</sup> B. A. Harmon,<sup>(1)†</sup> R. Knop,<sup>(1)</sup> C. Moisan,<sup>(2)‡</sup>  
R. Roy,<sup>(2)</sup> and R. G. Stokstad<sup>(1)</sup>

<sup>(1)</sup>*Nuclear Science Division, Lawrence Berkeley Laboratory, Berkeley, California 94720*

<sup>(2)</sup>*Laboratoire de physique nucléaire, Université Laval, Québec, P.Q., Canada G1K 7P4*

(Received 15 June 1990)

Cross sections for the multiple breakup of  $^{16}\text{O}$ ,  $^{14}\text{N}$ , and  $^{12}\text{C}$  projectiles scattered by an Au target were measured with an array of 34 phoswich detectors. The dissociation of the projectiles into as many as five charged particles has been observed. The yields of different exit channels correlate approximately with the threshold energy for separation of the projectile into the observed fragments. The excitation spectrum of the primary projectile-like nucleus was reconstructed from the measured positions and kinetic energies of the individual fragments. The energy sharing between projectile and target is consistent with a fast excitation mechanism in which differential increases in projectile excitation energy appear to be accompanied by comparable increases in target excitation. Calculations of the yields based on a sequence of binary decays are presented.

### I. INTRODUCTION

A heavy-ion collision can easily produce a nuclear system with an excitation energy so high that this excited object will decay by the emission of three, four, five, or even tens of particles and fragments before all the remnants are particle bound. However, a meaningful comparison with theory often requires a knowledge of the characteristics of the system before it disassembled—its charge and mass, its excitation energy, and its angular momentum. This problem of characterization generally can be solved if all the reaction products are detected, but the experimental problem is severe if there is a large number of particles involved and if some of them have low velocities. The present experimental study of multiparticle decay of a highly excited system solves the characterization problem by combining the following features: (i) a reaction mechanism that excites the system, in this case the projectilelike nucleus, without destroying its identity and (ii) a detector array with sufficient granularity and coverage to observe the fast forward-going particles from the breakup of the projectile. Thus, by studying the multiple breakup of excited projectilelike nuclei produced in peripheral reactions, we are able to detect all the relevant fragments and thereby characterize the excited system by its charge and excitation energy. A consequence of this completeness, however, is that the charge of the decaying system is relatively small: in our case the excited systems are carbon, nitrogen, and oxygen nuclei, produced by the scattering of beams of  $^{12}\text{C}$ ,  $^{14}\text{N}$ , and  $^{16}\text{O}$  at 32.5 MeV/nucleon by thin gold targets.

The motivation for the present experiment, to study the multiple decay of highly excited nuclei, has grown out of earlier studies of peripheral heavy-ion-induced reactions in which the emphasis was mainly on the two-body decays of a projectilelike excited system. Representative examples may be found in Refs. 1–3. Efficient

detection of multiple breakup requires the use of arrays of detectors, the development and use of which has increased rapidly in recent years.<sup>4–7</sup> The bombarding energy in the present experiment lies in the suspected “transition region,” that range of energy in which the phenomena of low-energy collisions, which are governed by the nuclear mean field, are expected to evolve into those characteristic of high-energy reactions, which are dominated by nucleon-nucleon collisions.<sup>8,9</sup> Another potential phenomenon of interest is “multifragmentation,” the simultaneous disintegration of a nucleus into three or more fragments, which has been predicted to occur at high excitation energies.<sup>10</sup>

After a brief description of the experimental apparatus and the analysis, we present the cross sections for the dissociation of the projectile into its constituent particles. The excitation energy of the projectilelike nucleus is then reconstructed. Under the assumption of a primary two-body process, the excitation energy sharing between the target and the projectile is obtained. Given the initial excitation energy of the decaying nucleus, it is possible with a statistical model to calculate the probability for decay into all allowed channels and to compare this with experiment. Following this, we summarize our conclusions. Brief accounts of portions of the present work have appeared elsewhere.<sup>11–14</sup>

### II. EXPERIMENT AND DATA ANALYSIS

The experiment was performed at the 88-Inch Cyclotron of the Lawrence Berkeley Laboratory. Beams of fully stripped  $^{16}\text{O}$ ,  $^{14}\text{N}$ , and  $^{12}\text{C}$  ions were produced in an Electron Cyclotron Resonance ion source and accelerated to an energy of 32.5 MeV/nucleon. Beam intensities were kept low (a few tenths of an electrical nanoampere) because of the high counting rates in the detectors closest to the beam. The gold target was 2-mg/cm<sup>2</sup> thick.

### A. Detector system

We used an array of 34 fast/slow plastic phoswich detectors.<sup>4</sup> Each element had the shape of a truncated pyramid [Fig. 1(a)], which permitted close packing. The front edge of a single element was 17 mm long and subtended an angle of 5°. An element consisted of a 1-mm thick fast scintillator (2 ns decay time) followed by 102 mm of a slow scintillator (225 ns). A photomultiplier tube was glued directly to the back of the slow plastic. Because each detector was tapered and viewed the target directly, the effective solid angle was independent of the particle range. Particles were identified by separately integrating the analog signal during a short and a long time gate. Protons and deuterons, and elements up to the charge of the projectile, could be resolved. The response for light and heavy ions is illustrated in Fig. 2. The spectrum was obtained at an average angle of 5°. The response and energy calibration of the detectors was determined by using four different beams ( $H_2^+$ ,  $^4He$ ,  $^{12}C$ , and  $^{16}O$ ). Different energies for each beam were obtained by degrading the 32.5-MeV/nucleon beam with appropriate foils. The light output was fitted with a different function of  $Z$  and energy for each detector. The energy resolution was better than 15% for all ions and about 3% for protons and alpha particles. The energy threshold for particle identification, indicated in Fig. 2, was due to the 1-mm  $\Delta E$  element, and increased gradually from 9 MeV/nucleon for  $Z=1$  and 2 to 19 MeV/nucleon for  $Z=8$ .

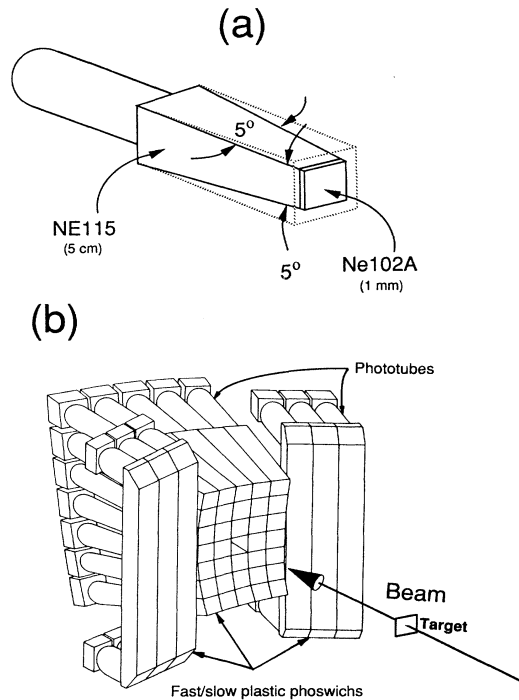


FIG. 1. (a) A single element of the array and (b) perspective view of the array. The detectors are mounted in a  $5 \times 7$  configuration with three position sensitive vertical strips on each side. The center is left open to allow the beam to go through the array when placed at zero degrees.

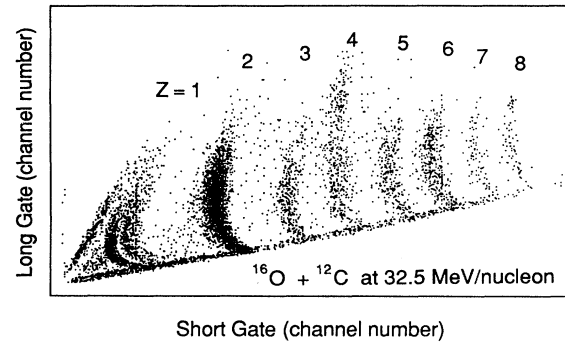


FIG. 2. Typical response for a single phoswich element. The light output in the short gate and in the long gate is determined by the energy deposited in the fast and slow elements, respectively.

The geometry of the array is illustrated in Fig. 1(b). A  $5 \times 7$  configuration, centered on the beam axis, was used in the present experiment. Three vertical strips of position sensitive plastic scintillator<sup>15</sup> were also mounted on each side of the array to extend the angular acceptance. The total area spanned by the 34-element array and the six strips corresponded to a rectangular cross-section of  $35^\circ \times 70^\circ$ . All coincidences between three or more particles were recorded, while those involving only one or two particles were scaled down by a factor of 128. Random coincidences were negligible.

### B. Selection of projectile breakup events

Events resulting from the breakup of the primary projectilelike nucleus were selected in the off-line analysis by requiring that the sum of the identified charge be equal to

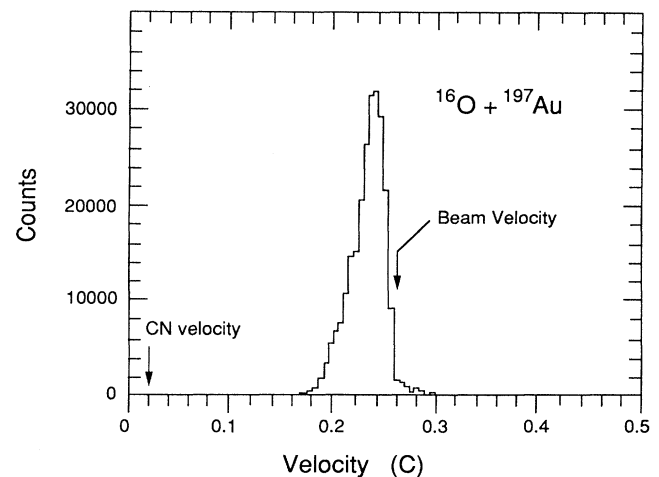


FIG. 3. The velocity  $V_{pp}$  of the projectilelike center of mass system, obtained from the sum of the momentum of each fragment (with charge  $Z_i$ ) divided by the mass of the projectile. To be included, an event must fulfill the condition  $\sum Z_i = Z_{proj}$ . Only events from the breakup channels ( $M \geq 2$ ) are shown. The beam velocity and the compound nucleus velocity are indicated by the arrows.

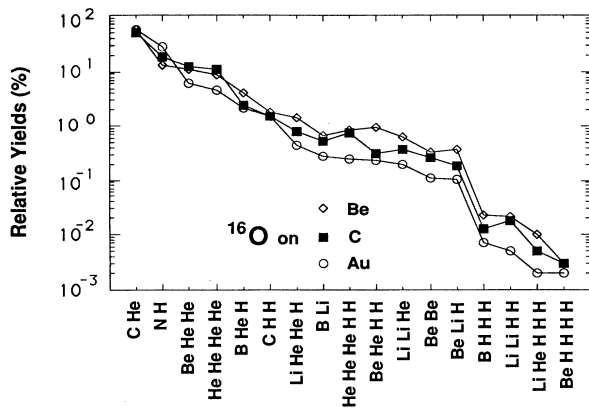


FIG. 4. Relative yields of different channels obtained for  $^{16}\text{O}$  bombarding targets of  $^9\text{Be}$ ,  $^{12}\text{C}$ , and  $^{197}\text{Au}$ . The events are selected according to the same requirements as in Fig. 3.

the charge of the projectile. This, and the energy threshold for particle identification set by the 1-mm thick fast plastic, effectively eliminated any contributions of low-energy particles (with  $Z \leq 2$ ) evaporated by an excited targetlike nucleus. The peripheral nature of the reaction was verified by observing that the velocities of all the detected fragments, including protons, were characteristic of the projectile and that the laboratory velocity,  $V_{pp}$ , of the center of mass system of the detected fragments

was close to the beam velocity (see Fig. 3). The peripheral nature of the reaction was also checked by observing that the relative yields of different channels were approximately independent of the target. This feature was demonstrated by making additional measurements on other targets.<sup>13</sup> Figure 4 shows the yields ordered by intensity for the different channels observed when a  $^{16}\text{O}$  beam interacts with targets of  $^{197}\text{Au}$ ,  $^{12}\text{C}$ , and  $^9\text{Be}$ .

For the special case of the decay of the projectilelike nucleus into two bodies, an insight into the interaction and decay mechanisms can be gained from the spatial distribution of one of the particles in coincidence with another detected at a fixed angle.<sup>1,2</sup> Figure 5 shows the angular correlation of alpha particles (contour lines) in coincidence with carbon ions detected at an average angle of  $5^\circ$ . The figure shows the actual coverage provided by the 40 detectors. The distribution is roughly centered on the reaction plane defined by the carbon nucleus and the beam axis. This pattern is indicative of a common source for the alpha particles and carbon nuclei, and is qualitatively consistent with the sequential decay of an excited oxygenlike nucleus<sup>16</sup> inelastically scattered at very forward angles and with an excitation energy peaked at about 11 MeV.

Different conclusions from different experiments can be found in the literature concerning the relative intensity of sequential or nonsequential components in two-body projectile fragmentation.<sup>17-19</sup> In Refs. 17 and 18 the heavy projectile fragment is detected at angles larger than the grazing angle, and a sequential model is fitted to events in

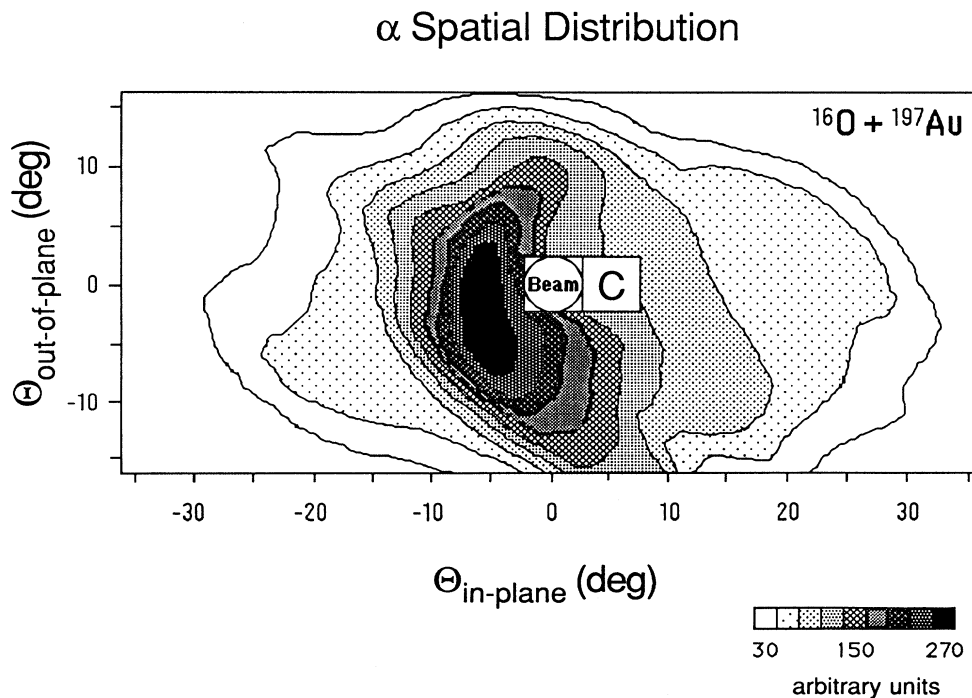


FIG. 5. Spatial correlation of He nuclei in coincidence with a carbon nucleus observed in a detector next to the beam. The out-of-plane angle is measured with respect to the median plane of the detector array, which contains the detected carbon nucleus. The in plane ( $\Theta_{\text{in-plane}}$ ) and out of plane ( $\Theta_{\text{out-of-plane}}$ ) angles are related to the polar angle ( $\Theta_{\text{lab}}$ ) of the  $\alpha$  particle (with respect to the beam) by  $\cos\Theta_{\text{lab}} = (\cos\Theta_{\text{in-plane}} \times \cos\Theta_{\text{out-of-plane}})$ .

which the projectile is scattered at primary angles well beyond the grazing angle. Comparison of the model with events corresponding to small primary angles then suggests the presence of a preequilibrium component in addition to a strong sequential component. Steckmeyer *et al.*<sup>19</sup> however conclude (for 60 MeV/nucleon Ar projectiles on Ag and Au target) that the observed events at small primary angles are predominantly sequential in nature. Since the grazing angle in the present experiment is 9° and the events shown in Fig. 5 correspond to primary angles near zero degrees, the present results are obtained in a qualitatively different kinematic region than the results of Refs. 17 and 18. Although our simulations of these data based on sequential decay are qualitatively consistent with the data, this does not rule out the presence of some preequilibrium component in this kinematic region or originating with larger primary scattering angles. The main point of Figs. 3–5 is to illustrate that we are observing fragments produced by the breakup of the projectile, since this is fundamental to our analysis.

### C. Efficiency

The close packing of the detectors in the array produced a high detection efficiency for particles from forward-peaked projectile breakup reactions. Nevertheless, it was possible for one or more fragments to miss the array. The relatively large effective angular coverage of the array for peripheral collisions, however, enabled us to determine empirically the efficiency for detecting a given breakup channel. For example, under the condition that the sum of all detected charges in an event equals the charge of the projectile ( $\sum Z = Z_{\text{proj}}$ ), more than 95% of the angular distribution of the heavy ions ( $Z \geq 3$ ) fell within the geometrical limit of the array. In fact, the main reason for missing a heavy ion was the 2.5° hole left open in the center of the array for the beam to exit. Angular distributions were also obtained for each channel for particles with  $Z \leq 2$ . Figure 6 shows the distribution of He particles produced in four different breakup channels of  $^{16}\text{O}$ . It is clear that He nuclei have similar angular distributions for all channels. Thus, the angular distribution of He particles in the C+He channel was almost the same as in the He+He+He+He channel. The same situation was also found for  $Z = 1$  particles. This suggests that the correlations among the particles in a given channel can be neglected when determining the efficiency of the array, and that the efficiency for a channel is well approximated by the product of the probabilities for detecting individually each of the fragments making up that channel. It is therefore possible to evaluate the probability of detecting a particular particle in a given channel by extrapolating the observed angular distribution for that particle into the regions not covered by the array. For example, in this way the overall detection efficiencies for the two-body channel C+He and the four-body channel Li+He+He+H, were estimated to be 67% and 32%, respectively. This procedure was checked in the case of the two-body channels by comparing the number of light particles observed in the vertical strips with the expectation based on the extrapolation of the angular distribu-

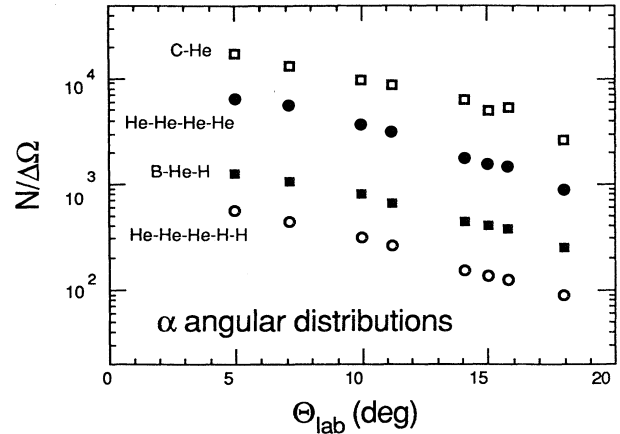


FIG. 6. Angular distribution of He nuclei from four different breakup channels. The vertical axis is in counts per steradian. The abscissa is the polar angle of the alpha particles with respect to the beam, which is different from the abscissa in Fig. 5.

tions measured with the 34-element array.

Efficiencies were also determined theoretically by simulating the sequential decay of an equilibrated projectile with the Monte Carlo code LILITA.<sup>16</sup> The angular distribution of the source (the excited primary projectile) was chosen to be the same as the measured<sup>20</sup> inelastic scattering of the projectile. The simulation included the geometry of the array (the center hole and all individual detectors) as well as the energy thresholds. This study showed that the effects of correlations were small and that double hits (two particles hitting the same detector element), with the exception of alpha particles generated by the decay of  $^8\text{Be}(g.s.)$ , could be neglected. The empirical efficiencies were well reproduced for those channels in which all fragments had masses equal to or greater than 4. The theoretical efficiencies for channels containing hydrogen isotopes, however, were too small because the protons were predicted to have broader angular distributions than observed. The use of empirical efficiencies, instead of the theoretical ones discussed above, reduces the dependence of the deduced cross sections on the choice of a model for the reaction.

## III. RESULTS

### A. Channel cross sections

The deduced cross sections for the different channels for each of the three beams ( $^{16}\text{O}$ ,  $^{14}\text{N}$ , and  $^{12}\text{C}$ ) are plotted in Fig. 7 as a function of the separation energy ( $Q_0$ ) for that channel. The channels and their  $Q_0$  values are given in the table adjacent to the figure. The absolute normalization (corrected for efficiency) was established by comparison of the measured elastic scattering to the Rutherford cross section and also by comparing the inclusive yields of heavy ions to those measured with a solid-state detector in an earlier experiment.<sup>20</sup> The two determinations were in good agreement; the systematic

error on the absolute normalization was estimated to be 20%.

The channels shown in Fig. 7 are distinguished experimentally only by their combinations of atomic numbers. For example, the contributions of  $^{12}\text{B}+^3\text{He}+p$  and  $^{10}\text{B}+^4\text{He}+d$  are summed together and are plotted against the least negative of the two  $Q_0$  values,  $-23.1$  MeV. The detection of  $^8\text{Be}$  poses an additional complication in that there is a 60% probability that the two  $^4\text{He}$  nuclei from the decay of a  $^8\text{Be}(g.s.)$  nucleus will hit the same detector. Such double hits were identified as  $Z=4$  and were not distinguished from  $^{7,9}\text{Be}$ . Therefore, we have summed all events which differed only by two  $Z=2$  fragments or one  $Z=4$  fragment (such as  $\text{He}+\text{He}+\text{He}+\text{He}$ ,  $\text{He}+\text{He}+\text{Be}$ , and  $\text{Be}+\text{Be}$ ) and plotted them versus the most positive  $Q_0$  value. These channels are indicated by an arrow in Fig. 7.

It is interesting to note that the cross section for the breakup into three or more charged particles accounts for 26% and 24% of the total  $^{16}\text{O}$  and  $^{14}\text{N}$  breakup cross section, respectively. This ratio goes up to 55% for the breakup of  $^{12}\text{C}$ . This is because the most dominant

charged particle breakup channel is  $\text{He}+\text{He}+\text{He}$  (of course, this decay may proceed partly via the intermediate state,  $^4\text{He}+^8\text{Be}$ ). This channel alone represents 49% of the total  $^{12}\text{C}$  breakup cross section.

The logarithm of the cross section (Fig. 7) has an approximately linear relationship with  $Q_0$  over a range of 3 to 4 orders of magnitude in yield. The correlation with  $Q_0$  is much stronger than the correlation with particle multiplicity. Cross sections for breakup into specific exit channels can be characterized approximately by a slope parameter,  $E_0$ , which has values of 6.4, 5.5, and 6.0 MeV ( $\pm 0.4$ ) for  $^{16}\text{O}$ ,  $^{14}\text{N}$ , and  $^{12}\text{C}$ , respectively. This exponential dependence provides the justification for plotting the cross sections versus the most positive  $Q_0$  value.

### B. Excitation energies of the primary nuclei

The excitation energy spectrum of the primary projectilelike nuclei prior to their decay was determined event by event from the position and energy of each of the detected particles under the assumption that the particles originate from the projectile. The relative kinetic energy of the fragments in the center of mass system of the primary projectilelike nucleus is given by

$$K_{\text{rel}} = \frac{1}{2} \sum_i m_i (\mathbf{V}_i - \mathbf{V}_{pp})^2, \quad (1)$$

where  $\mathbf{V}_i$  is the laboratory velocity of a fragment. For  $Z \geq 2$ , the mass of the fragment  $m_i$  was taken as the most abundant isotope. These values are very close to the average mass measured with a silicon telescope in coincidence with the array. The laboratory velocity of the projectilelike center of mass system  $\mathbf{V}_{pp}$  was defined by  $\mathbf{V}_{pp} = 1/M_p \sum \mathbf{P}_i$ , where  $M_p$  is the mass of the projectile. The excitation energy of the primary projectilelike nucleus is then

$$E_{pp}^* = K_{\text{rel}} - Q_0, \quad (2)$$

where  $Q_0$  is the appropriate  $Q$  value for that breakup channel. Residual excitation energies of bound fragments were neglected. The exact position of a recorded particle was chosen at random over the face of the detector. A correction was made for the different isotopic compositions of a given channel by estimating the yields of each isotopic combination using the above slope parameters and a weighting factor based on  $\exp(Q_0/E_0)$ . A weighted fraction of events was then offset to the more negative  $Q_0$  value associated with that isotopic combination. Figure 8 shows the resulting primary excitation spectrum for  $^{16}\text{O}$ . Contributions from some individual channels are also shown.

The slow component of the light produced by two alpha particles in the same detector is slightly larger than for a hypothetical stable  $^8\text{Be}$  nucleus. These double-hit events can be seen in the  $Z=4$  band in Fig. 2. The fast component of the light output (corresponding mainly to the  $\Delta E$  portion of the phoswich) for a double alpha particle or a  $^9\text{Be}$  event cannot be distinguished. The energy calibration interpolated for  $Z=4$  particles thus overestimates by about 30% the energy of two alpha particles detected simultaneously. However, we estimate that dou-

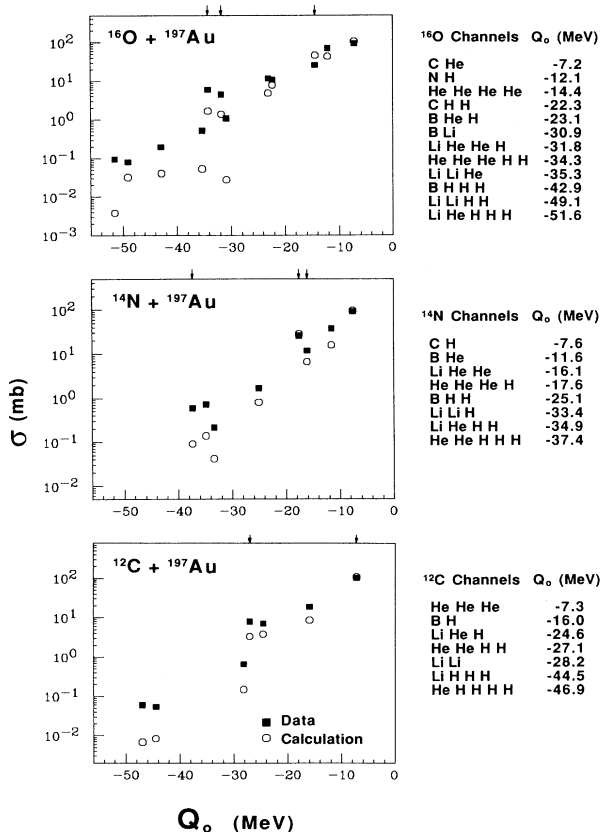


FIG. 7. Cross sections for breakup channels plotted versus the most positive  $Q_0$  value of all isotopic combinations consistent with the elements making up that channel. The channels containing a combination of two helium nuclei or a Be nucleus have been summed and are indicated by an arrow. The open circles show the results of a statistical decay calculation (Refs. 11 and 26).

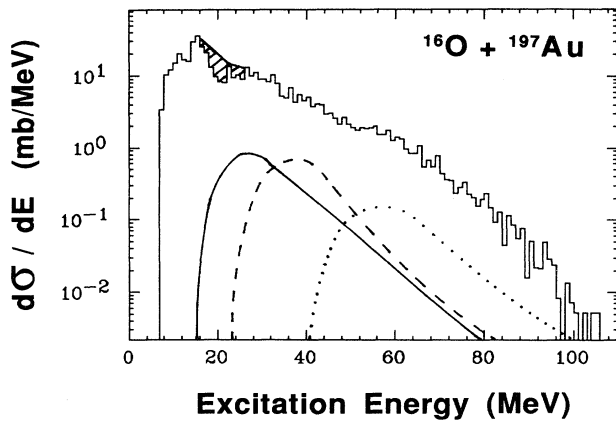


FIG. 8. The excitation energy spectrum of the primary projectilelike nucleus for the system  $^{16}\text{O} + ^{197}\text{Au}$ . The solid, dashed, and dotted lines represent contributions of the channels  $\text{He} + \text{He} + \text{He} + \text{He}$ ,  $\text{C} + \text{H} + \text{H}$ , and  $\text{He} + \text{He} + \text{He} + \text{H} + \text{H}$ , respectively. The hatched area represents the estimated contribution of the undetected channel  $^{15}\text{O} + \text{n}$ . The spectra for the other projectiles were qualitatively similar.

ble hits resulting from  $^8\text{Be}$  contribute about 15% or less to the channels indicated by the arrows in Fig. 7. Since these channels represent a small fraction of the total projectile breakup cross section, the error in the total excitation energy spectrum introduced by the different light-to-energy conversion factors for two alpha particles and a Be nucleus is small.

Due to the very low efficiency of the detectors for free neutrons, the breakup of the projectile into a channel containing only one charged particle and one or more neutrons will not be included in this spectrum because of the trigger requirement that there be at least a double coincidence. The contribution of the undetected channel  $^{15}\text{O} + \text{n}$  was estimated by taking the shape of the excitation spectrum from that of  $\text{N} + \text{H}$ , normalizing the total yield according to the empirical dependence on  $Q_0$ , and shifting the spectrum by the difference in the  $Q_0$  and Coulomb barrier values. The estimated additional contribution of this channel is indicated by the hatched area in Fig. 8.

Neutrons may also be picked up by the projectile, and pickup reactions are known to produce a generally higher excitation energy in the projectilelike nucleus than does inelastic scattering. The pickup reaction  $^{197}\text{Au}(^{16}\text{O}, ^{17}\text{O}^*)$  has been studied recently by Gazes *et al.*<sup>21</sup> and shown to populate the channels  $^{13}\text{C} + ^4\text{He}$  and  $^{12}\text{C} + ^4\text{He} + \text{n}$ . These channels are not distinguished and were included in the  $\text{C} + \text{He}$  channel along with  $^{12}\text{C} + ^4\text{He}$ . We have simulated the effect of neutron pickup and decay using a statistical decay model and found that even a level of neutron pickup equal to the intensity of the inelastic scattering does not reproduce the experimental yields for channels with very negative  $Q_0$  values. Thus it appears that neutron pickup is at most a partial explanation for the events corresponding to high projectile excitation energies.

There are also reaction mechanisms that may contribute to our experimental results, however, that does not

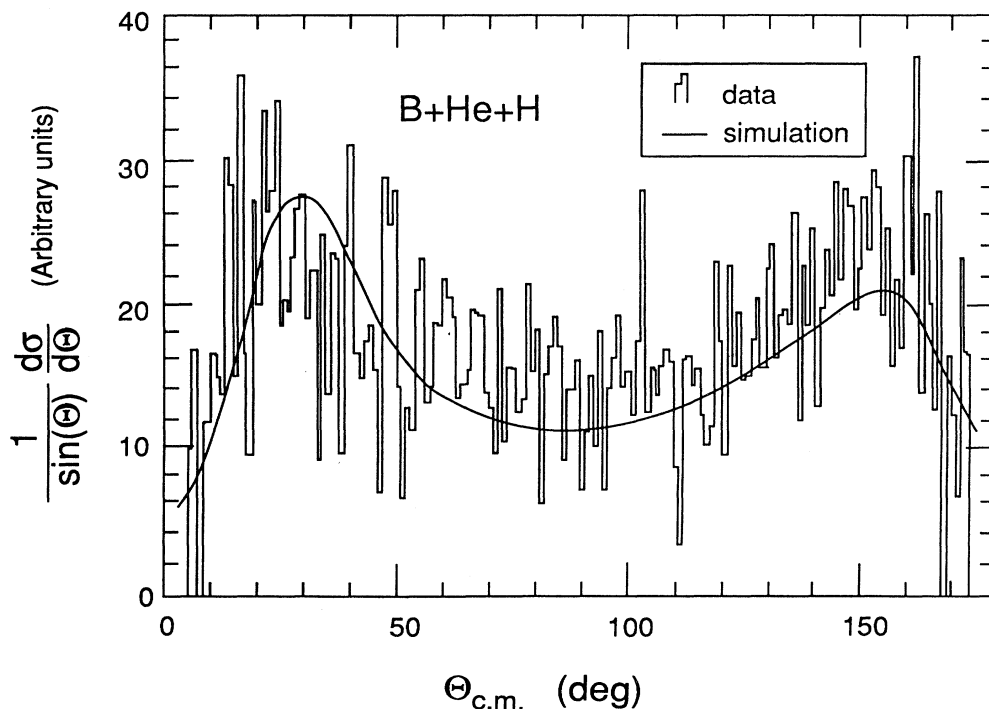


FIG. 9. Angular distribution of He nuclei in the center-of-mass system for the  $\text{B} + \text{He} + \text{H}$  channel.  $\Theta_{\text{c.m.}} = 0^\circ$  corresponds to the direction of the primary  $^{16}\text{O}$ . The smooth line represents the result of a Monte Carlo simulation based on an isotropic angular distribution and filtered for the experimental conditions.

strictly satisfy the assumption that all of the detected fragments originate solely from the decay of the projectile. Preequilibrium emission of protons from the region of overlap between projectile and target is an example of this and might be responsible for the observed forward-peaked angular correlation of the protons relative to the expectation for sequential decay. Another example could be final-state interactions between fragments of the projectile and the target, which alter the directions of the fragments and thereby change the relative kinetic energy and deduced excitation energy. (Final-state interactions will not affect that portion of the projectile excitation energy associated with the  $Q_0$  value for that channel, however.) To investigate this question, we made a Monte Carlo simulation of the sequential decay of an equilibrated projectilelike nucleus with the code LILITA<sup>16</sup> (see Sec. II C). In the projectilelike center of mass, fragments were emitted sequentially with an isotropic angular distribution and interactions with the target were neglected. After filtering the calculated events under identical experimental conditions, the resulting angular distribution was compared to the data. Figure 9 shows the He angular distribution from the channel B-He-H. This channel has been chosen for its high excitation energy in  $^{16}\text{O}$  (greater than 23 MeV) and sufficient counting statistics. The simulation is in good agreement with the data, implying that a large majority of He particles are emitted sequentially in the projectilelike nucleus center of mass. Thus, no evidence for final-state interactions with the target was found in the He angular distributions. This is consistent with a simple statistical estimate<sup>22</sup> for the lifetime of the excited  $^{16}\text{O}$  nucleus ( $10^{-21}$  sec at 32 MeV excitation), during which time the projectile travels about 100 fm.

### C. Excitation energy sharing

The distribution of excitation energy between the projectile and the target is an indication of the degree of thermal equilibrium reached.<sup>23</sup> When the interaction time is long enough for the target and projectile to reach thermal equilibrium, the total excitation energy is shared according to the ratio of their masses. On the other hand, in a fast process involving collisions of nucleons in the projectile with those in the target, the excitation energy will be shared equally, on the average, between the projectile and target. The latter is what one would expect for peripheral collisions at intermediate and high energies.

In the preceding section, we deduced the excitation energy of the projectile under certain assumptions. The same assumptions allow us to deduce the excitation energy of the targetlike nucleus as well. It is given by

$$E_T^* = E_{\text{Beam}} - K_{pp} - K_T - E_{pp}^* \quad (3)$$

where  $K_{pp}$  is the kinetic energy of the primary projectilelike nucleus obtained from  $V_{pp}$  and  $K_T$  is the kinetic energy of the targetlike nucleus, evaluated from the conservation of momentum,

$$\mathbf{P}_{\text{Beam}} = \mathbf{P}_T + \mathbf{P}_{pp} \quad (4)$$

$\mathbf{P}_{\text{Beam}}$ ,  $\mathbf{P}_T$ , and  $\mathbf{P}_{pp}$  are, respectively, the momentum of the beam, the recoiling targetlike nucleus, and the projectilelike nucleus. The result of this event-by-event determination of the energy sharing is given in Fig. 10, which shows the excitation energy correlation between the targetlike and the projectilelike nucleus for two systems,  $^{16}\text{O} + ^{197}\text{Au}$  [Fig. 10(a)] and  $^{14}\text{N} + ^{197}\text{Au}$  [Fig. 10(b)]. The solid line on the left indicates the limit of a fully damped reaction where the target and the projectile had sufficient time during the interaction to reach thermal equilibrium. If the parameter  $d$ , used to calculate the level density parameter  $a = A/d$ , is the same for the targetlike and the projectilelike nucleus, then the relation  $E^* = aT^2$  results in an energy sharing corresponding to the ratio of their masses.<sup>23</sup> Note that very high excitation energies cannot be reached in the projectile in this case because the mass asymmetry favors the target by 12:1 for an  $^{16}\text{O}$  projectile and by 14:1 for an  $^{14}\text{N}$  projectile. The other line represents an equal sharing of energy associated with a fast projectile-target interaction. For instance, a bidirectional exchange of one or more nucleons would result in such a sharing.

The contour lines show the experimental results when all observed channels are summed. Since the cross sec-

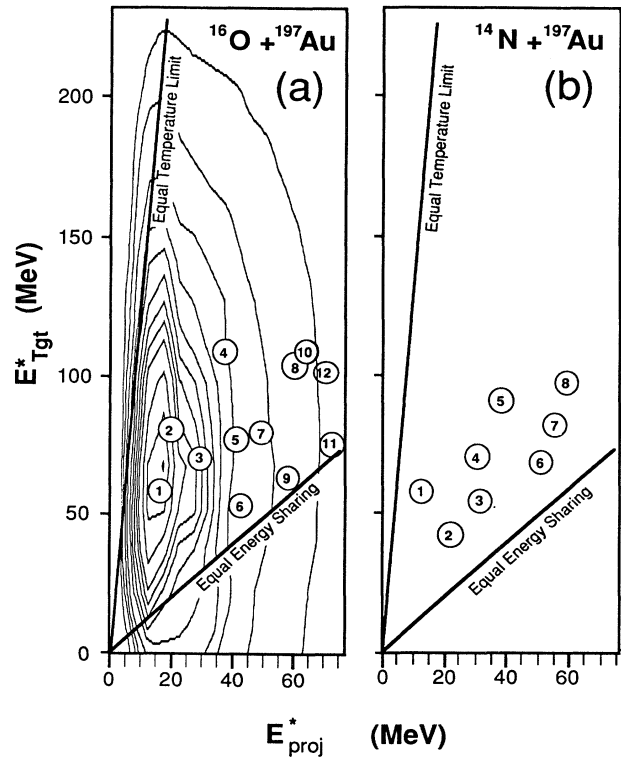


FIG. 10. (a) Excitation energy of the projectilelike nucleus as a function of the target excitation energy. The fully damped reaction (equal temperature limit) and fast reaction (equal energy sharing) are indicated by the two oblique lines. The numbered open circles show the average value for each channel individually. The numbers labeling the data points are defined in Table I. The channels in the table are ordered by decreasing  $Q$  value (see also Fig. 7). (b) Same as (a) for the reaction  $^{14}\text{N} + ^{197}\text{Au}$ .

tions for the different channels vary by orders of magnitude, the contour lines are dominated by the two or three most probable channels. The numbered circles represent the average value for each individual channel. The channels are ordered as in Fig. 7 and Table I by increasing negative  $Q_0$  value, i.e., by increasing separation energy. The ratios  $R \equiv E_{\text{tgt}}^*/E_{\text{proj}}^*$  for the individual channels are presented in Table I. The error bars reflect the range of variation of the ratio calculated from the FWHM of the excitation energy spectra. For the  $^{14}\text{N}+^{197}\text{Au}$  system, the energy-sharing ratio for the channel 1 (C+H) has also been obtained by Pruneau *et al.*<sup>24</sup> for a higher beam energy, 40 MeV/nucleon. The values of the ratio obtained at the two different energies overlap slightly. On the average, the ratios become closer to unity as the separation energy increases. The reason for the larger ratios at the lower separation energies is that the projectiles with high excitation energies (and, therefore, with excitation energy ratios closer to unity) decay preferentially into channels with larger numbers of fragments and hence larger separation energies.

It is important to note that the increase in average excitation energy in the projectile as one goes from channel 1 to channel 12 [see Fig. 10(a)], is about the same ( $\sim 50$  MeV) as it is in the target. These approximately equal *incremental* increases in the excitation energy in the projectile and in the target suggest that nucleon-nucleon collisions (or exchanges) are becoming an important mechanism for inducing excitation in projectile breakup reactions. Thus, the changes in average excitation energies that can be obtained from Table I and Fig. 10 are characteristic of quasielastic reactions and do not themselves

suggest any significant equilibration of energy between target and projectile. This is as expected for these reactions with a light projectile and with the requirement that no net charge be transferred.

#### IV. STATISTICAL DECAY CALCULATION

A standard interpretation of projectile breakup consists of factoring the reaction into two independent stages—a fast excitation process followed by decay. The decay may be slow and involve a series of sequential, binary decays. Or the decay may be prompt, implying that the breakup of the projectile occurs while it is still in the vicinity of the target or that its dissociation into three or more fragments occurs more or less simultaneously regardless of location (multifragmentation). It is possible, within this standard interpretation, to analyze the reaction by making use of the primary spectrum deduced from experiment and a model for the second stage. An analysis of the directional correlations among the particles in a given channel, using the kinematic models of Lopez and Randrup<sup>25</sup> for multifragmentation and for sequential decay is reported elsewhere<sup>12</sup> for these experimental data. Here we analyze the relative yields of the different channels by comparing a statistical calculation<sup>26</sup> for multiple sequential binary splits with the data.

At each stage of the cascade, all energetically allowed splits are considered. The available excitation energy  $U$  at the saddle point for a split into two nuclei is given by

$$U_i = E^* + Q_0 - V_b \quad (5)$$

where  $E^*$  is the excitation energy with respect to the ground state,  $-Q_0$  is the separation energy for channel  $i$ , and  $V_b$  is the Coulomb barrier in the saddle-point configuration. The decay widths  $\Gamma_i$  for different channels  $i$  are then calculated from a comparison of the densities of states at the saddle points.

$$\Gamma_i = (T/2\pi)(E^*/U_i)^2 [\exp(2\sqrt{aU_i})/\exp(2\sqrt{aE^*})], \quad (6)$$

where  $T = \sqrt{E^*/a}$  is the temperature. From the available energy, an energy equal to twice the temperature is taken for the relative kinetic energy ( $E_k$ ) of the daughter nuclei, provided  $U > 2T$ . If  $U < 2T$ , all of the available energy goes into kinetic energy. The excess energy ( $U - 2T$ ) available for excitation in the daughter nuclei is then shared according to their mass ratio. Some deviations from a proportional division of excitation energy are necessary, for instance, because protons and neutrons cannot carry excitation energy, and light nuclei that have no states below their lowest threshold for particle decay cannot have an amount of excitation energy less than this threshold. This calculation is similar to one described by Auger *et al.*,<sup>27</sup> with the exception that ground-state masses are used throughout and rotational energy is neglected. A principal feature of the present calculation is that, in any binary split, each of the fragments may undergo further decay.

The results of the calculation are shown in Fig. 7. The distribution of excitation energy of the nuclei before de-

TABLE I. Energy sharing ratios.

Energy Sharing $R$		$E_{\text{tgt}}^*/E_{\text{proj}}^*$	
$^{16}\text{O}$ channels			
(1)	C He	3.5	$\pm 0.8$
(2)	N H	4.5	0.8
(3)	He He He He	2.5	0.9
(4)	C H H	3.0	0.5
(5)	B He H	1.9	0.7
(6)	B Li	1.3	0.5
(7)	Li He He H	1.6	0.4
(8)	He He He H H	1.8	0.4
(9)	Li Li He	1.1	0.4
(10)	B H H H	1.8	0.5
(11)	Li Li H H	1.1	0.5
(12)	Li He H H H	1.6	0.5
$^{14}\text{N}$ channels		$E_{\text{tgt}}^*/E_{\text{proj}}^*$	
(1)	C H	4.6	$\pm 0.9$
(2)	B He	2.1	0.7
(3)	Li He He	1.9	0.6
(4)	He He He H	2.4	0.5
(5)	B H H	2.5	0.6
(6)	Li Li H	1.4	0.4
(7)	Li He H H	1.5	0.4
(8)	He He H H H	1.7	0.4



cay was taken from experiment and individual channels having the same combination of atomic numbers are summed to compare with the data. The calculation compares favorably with experimental results for  $Q_0$  values extending down to 30 MeV, which accounts for most of the cross section, but the yields at more negative  $Q_0$  values are poorly reproduced, with the calculated values being low by factors of 5 to 20. We have also made similar calculations with LILITA<sup>16</sup> (which includes angular momentum and the effects of discrete excited states, but considers the decay of the heavier object only) and obtained qualitatively similar results. The possibility that neutron pickup might produce large excitation energies (and thereby increase the yield of the channels with  $Q_0 < -30$  MeV) was considered in Sec. III B and seems unlikely. At present, the origin of this discrepancy between theory and experiment is not understood.

### V. SUMMARY

In summary, the cross sections for the breakup of  $^{16}\text{O}$ ,  $^{14}\text{N}$ , and  $^{12}\text{C}$  projectiles into a large number of exit channels, some having as many as five charged particles, have been measured with an array of 34 plastic scintillators. This has enabled a more global examination of the breakup of the projectile than would be possible with two-particle coincidence experiments. The relative yields of the different channels were observed to correlate approximately with the threshold energy for separation of projectile into the detected fragments. The excitation spectrum of the primary projectilelike nucleus, deduced from the separation energies and the measured positions and kinet-

ic energies of the individual fragments, has a maximum at low excitation energies, but also extends to quite high excitation energies (5–6 MeV/nucleon). A Monte Carlo simulation of the B+He+H channel, which is produced by the decay of  $^{16}\text{O}$  nuclei at excitation energies greater than 23 MeV, shows no evidence for final-state interactions between fragments of the projectile and the Coulomb field of the target. The sharing of the excitation energy between the projectilelike nucleus and the target does not indicate any evidence for strong equilibration in the initial stage of the reaction and is thus consistent with a fast excitation process. The yields of the light particles are compared with the predictions of multiple sequential decay models. These models were found to underestimate the yields of the channels populated by the decay of the highest excitation energies in the projectile and the yields of protons at forward angles. With these exceptions, the statistical models, including the sphericity-coplanarity analysis presented in Ref. 12, show good agreement for the multiple decay properties of the excited projectilelike nuclei studied in the present reactions.

### ACKNOWLEDGMENTS

The authors express their gratitude to E. Plagnol, L. Potvin, and C. Rioux for their help during the experiment, and to J. A. Scarpaci for performing statistical model simulations for the binary channels. This work was supported by the U.S. Department of Energy under Contract DE-AC03-76SF00098 and by the National Science and Engineering Research Council of Canada.

\*Present address: Laboratoire de physique nucléaire, Université Laval, Québec, P.Q., Canada G1K 7P4.

†Present address: Space Science Lab., Nasa/Marshall Space Flight Center, Huntsville, AL 35812.

‡Present address: Université de Montréal, C.P. 6128 Station A 2905 Chemin des services, Montréal, Quebec, Canada H3C 3J7.

<sup>1</sup>W. D. M. Rae, A. J. Cole, A. Dacal, R. Legrain, B. G. Harvey, J. Mahoney, M. J. Murphy, R. G. Stokstad, and I. Tserruya, *Phys. Lett.* **105B**, 417 (1981); *Phys. Rev. C* **30**, 158 (1984).

<sup>2</sup>H. Homeyer, M. Bürgel, M. Clover, Ch. Egelhaaf, H. Fuchs, A. Gamp, D. Kovar, and W. Rauch, *Phys. Rev. C* **26**, 1335 (1982).

<sup>3</sup>R. H. Siemssen, G. J. Balster, H. W. Wilshut, P. D. Bond, P. C. Crouzen, P. B. Goldhoorn, S. Han, and Z. Sujkowski, *Phys. Lett.* **161B**, 261 (1985).

<sup>4</sup>J. Pouliot, Y. Chan, A. Dacal, A. Harmon, R. Knop, M. E. Ortiz, E. Plagnol, and R. G. Stokstad, *Nucl. Instrum. Methods* **A270**, 69 (1988).

<sup>5</sup>R. Bougault, D. Horn, G. C. Ball, M. G. Steer, and L. Potvin, *Nucl. Instrum. Methods* **A245**, 455 (1986).

<sup>6</sup>D. G. Sarantites, L. G. Sobotka, T. M. Semkow, V. Abenante, J. Elsen, J. T. Hood, Z. Li, N. G. Nicolis, D. W. Stracener, J. Valdes, and D. C. Hensley, *Nucl. Instrum. Methods* **A264**, 319 (1988); D. W. Stracener, D. G. Sarantites, L. G. Sobotka, J. Elson, J. T. Hood, Z. Majka, V. Abenante, A. Chbihi, and D. C. Hensley, *Nucl. Instrum. Methods* (to be published).

<sup>7</sup>R. T. de Souza, N. Carlin, Y. D. Kim, J. Ottarson, L. Phair, D. R. Bowman, C. K. Gelbke, W. G. Gong, W. G. Lynch, R. A. Pelak, T. Peterson, G. Poggi, M. B. Tsang, and H. M. Xu, Michigan State University Report MSUCL-720, 1990 (unpublished).

<sup>8</sup>R. G. Stokstad, *Comments Nucl. Part. Phys.* **13**, 231 (1984).

<sup>9</sup>R. Dayras, *J. Phys. Colloq.* **47**, C4-13 (1986).

<sup>10</sup>J. Bondorf, R. Donangelo, I. Mishustin, C. Pethick, H. Schulz, and K. Sneppen, *Nucl. Phys.* **A442**, 321 (1985); J. Bondorf, R. Donangelo, H. Schulz, and K. Sneppen, *Phys. Lett.* **162B**, 30 (1985); D. H. E. Gross, Zhang Xiao-ze, and Xu Shu-yan, *Phys. Rev. Lett.* **56**, 1544 (1986).

<sup>11</sup>J. Pouliot, Y. Chan, A. Dacal, D. E. DiGregorio, B. A. Harmon, R. Knop, M. E. Ortiz, E. Plagnol, R. G. Stokstad, C. Moisan, L. Potvin, C. Rioux, and R. Roy, *Phys. Lett. B* **223**, 16 (1989).

<sup>12</sup>B. A. Harmon, J. Pouliot, J. A. Lopez, J. Suro, R. Knop, Y. Chan, D. E. DiGregorio, and R. G. Stokstad, *Phys. Lett. B* **235**, 234 (1990).

<sup>13</sup>R. G. Stokstad, in *Proceedings of the XX International Summer School on Nuclear Physics*, Mikotajki, Poland (IOP, England, 1989).

<sup>14</sup>J. Pouliot, Y. D. Chan, A. Dacal, D. E. DiGregorio, B. A. Harmon, R. Knop, M. E. Ortiz, E. Plagnol, R. G. Stokstad, C. Moisan, L. Potvin, C. Rioux, and R. Roy, *Conference Proceedings of the Symposium on Nuclear Dynamics and Nuclear Disassembly*, ACS, Dallas, Texas (World Scientific,

- Teaneck, N.J., 1989).
- <sup>15</sup>H. R. Schmidt, M. Bantel, Y. D. Chan, S. B. Gazes, S. Wald, and R. G. Stokstad, *Nucl. Instrum. Methods* **A242**, 111 (1985).
- <sup>16</sup>J. Gomez del Campo and R. G. Stokstad, Report LILITA, ORNL-Tm-7295, 1981 (unpublished).
- <sup>17</sup>J. Uckert, A. Budzanowski, M. Bürgel, H. Fuchs, H. Homeyer, and W. Terlau, *Phys. Lett. B* **206**, 190 (1988); K. Möhring, T. Srokowski, D. H. E. Gross, and H. Homeyer, *ibid.* **B 203**, 210 (1988).
- <sup>18</sup>P. L. Gonthier, P. Harper, B. Bouma, R. Ramaker, D. A. Cebra, Z. M. Koenig, D. Fox, and G. D. Westfall, *Phys. Rev. C* **41**, 2635 (1990); P. L. Gonthier, B. Bouma, P. Harper, R. Ramaker, D. A. Cebra, Z. M. Koenig, D. Fox, and G. D. Westfall, *ibid.* **35**, 1946 (1987).
- <sup>19</sup>J. C. Steckmeyer, G. Bizard, R. Brou, E. Eudes, J. L. Laville, J. B. Natowitz, J. P. Patry, B. Tamain, A. Thiphagne, H. Doubre, A. Pégahaire, J. Peter, E. Rasato, J. C. Adloff, A. Kamili, G. Rudolf, F. Scheibling, F. Guibault, C. Lebrun, and F. Hanappe, *Nucl. Phys.* **A500**, 372 (1989).
- <sup>20</sup>M. E. Ortiz, E. Chavez-Lomeli, A. Dacal, Y. D. Chan, S. B. Gazes, B. A. Harmon, J. Pouliot, and E. Plagnol, *Notas de Fisica*, proceedings of the XI Oaxtepec Symposium of Nuclear Physics, Oaxtepec, Morelos, Mexico, 1988 (unpublished), p. 235.
- <sup>21</sup>S. B. Gazes, Y. D. Chan, E. Chavez, A. Dacal, M. E. Ortiz, K. Siwek-Wilczynska, J. Wilczynski, and R. G. Stokstad, *Phys. Lett. B* **208**, 194 (1988).
- <sup>22</sup>D. Shapira, R. G. Stokstad, and D. A. Bromley, *Phys. Rev. C* **10**, 1063 (1974).
- <sup>23</sup>H. Sohlbach, H. Freiesleben, W. F. W. Schneider, D. Schüll, P. Braun-Munzinger, B. Kohlmeyer, M. Marinescu, and F. Pühlhofer, *Nucl. Phys.* **A467**, 349 (1987).
- <sup>24</sup>C. Pruneau, L. Potvin, R. Roy, C. St-Piere, G. C. Ball, R. Bougault, E. Hagberg, D. Horn, D. Cebra, D. Fox, and G. D. Westfall, *Nucl. Phys.* **A500**, 168 (1989).
- <sup>25</sup>J. Lopez and J. Randrup, *Nucl. Phys.* **A491**, 477 (1989).
- <sup>26</sup>R. Knop and R. G. Stokstad, LBL Report 26439, 1988 (unpublished).
- <sup>27</sup>F. Auger, B. Berthier, A. Cunsolo, A. Foti, W. Mittig, J. M. Pascaud, E. Plagnol, J. Québert, and J. P. Wieleczko, *Phys. Rev. C* **35**, 190 (1987).